tvst

Article

Oculomotor Responses to Dynamic Stimuli in a 44-Channel Suprachoroidal Retinal Prosthesis

Samuel A. Titchener[1,2], Jessica Kvansakul[1,2], Mohit N. Shivdasani[3,1], James B. Fallon[1,2], D. A. X. Nayagam[1,4], Stephanie B. Epp[1], Chris E. Williams[1,2], Nick Barnes[5,6], William G. Kentler[7], Maria Kolic[8], Elizabeth K. Baglin[8], Lauren N. Ayton[8–10], Carla J. Abbott[8,9], Chi D. Luu[8,9], Penelope J. Allen[8,9], and Matthew A. Petoe[1,2]

[1] Bionics Institute, East Melbourne, Australia
[2] Medical Bionics Department, University of Melbourne, Melbourne, Australia
[3] Graduate School of Biomedical Engineering, University of New South Wales, Kensington, Australia
[4] Department of Pathology, University of Melbourne, St. Vincent's Hospital, Melbourne, Australia
[5] Data61, CSIRO, Canberra, Australia
[6] Research School of Engineering, Australian National University, Canberra, Australia
[7] Department of Biomedical Engineering, University of Melbourne, Melbourne, Australia
[8] Centre for Eye Research Australia, Royal Victorian Eye & Ear Hospital, Melbourne, Australia
[9] Ophthalmology, Department of Surgery, University of Melbourne, Melbourne, Australia
[10] Department of Optometry and Vision Sciences, University of Melbourne, Melbourne, Australia

Correspondence: Samuel A. Titchener, Bionics Institute, 384-388 Albert St, East Melbourne 3002, Australia. e-mail: stitchener@bionicsinstitute.org

Received: June 19, 2020
Accepted: November 12, 2020
Published: December 18, 2020

Keywords: visual prosthesis; retinal prosthesis; motion perception; eye movements; head movements

Citation: Titchener SA, Kvansakul J, Shivdasani MN, Fallon JB, Nayagam DAX, Epp SB, Williams CE, Barnes N, Kentler WG, Kolic M, Baglin EK, Ayton LN, Abbott CJ, Luu CD, Allen PJ, Petoe MA. Oculomotor responses to dynamic stimuli in a 44-channel suprachoroidal retinal prosthesis. Trans Vis Sci Tech. 2020;9(13):31, https://doi.org/10.1167/tvst.9.13.31

Purpose: To investigate oculomotor behavior in response to dynamic stimuli in retinal implant recipients.

Methods: Three suprachoroidal retinal implant recipients performed a four-alternative forced-choice motion discrimination task over six sessions longitudinally. Stimuli were a single white bar ("moving bar") or a series of white bars ("moving grating") sweeping left, right, up, or down across a 42″ monitor. Performance was compared with normal video processing and scrambled video processing (randomized image-to-electrode mapping to disrupt spatiotemporal structure). Eye and head movement was monitored throughout the task.

Results: Two subjects had diminished performance with scrambling, suggesting retinotopic discrimination was used in the normal condition and made smooth pursuit eye movements congruent to the moving bar stimulus direction. These two subjects also made stimulus-related eye movements resembling optokinetic reflex (OKR) for moving grating stimuli, but the movement was incongruent with stimulus direction. The third subject was less adept at the task, appeared primarily reliant on head position cues (head movements were congruent to stimulus direction), and did not exhibit retinotopic discrimination and associated eye movements.

Conclusions: Our observation of smooth pursuit indicates residual functionality of cortical direction-selective circuits and implies a more naturalistic perception of motion than expected. A distorted OKR implies improper functionality of retinal direction-selective circuits, possibly due to retinal remodeling or the non-selective nature of the electrical stimulation.

Translational Relevance: Retinal implant users can make naturalistic eye movements in response to moving stimuli, highlighting the potential for eye tracker feedback to improve perceptual localization and image stabilization in camera-based visual prostheses.

Introduction

Visual prostheses attempt to restore some visual function to the profoundly vision impaired. To date, three visual prostheses have been granted regulatory approval; the Argus II epiretinal implant (Second Sight, Los Angeles, CA, USA),[1] the Alpha AMS subretinal implant (Retina Implant AG, Reutlingen, Germany),[2] and the IRIS II epiretinal implant (Pixium Vision, Paris, France).[3] Other implants are at the clinical trial stage, such as a second-generation suprachoroidal retinal implant (Bionic Vision Technologies, Melbourne, VIC, Australia) (Allen PJ. *IOVS*. 2020;61:ARVO Abstract 2200; Kolic M. *IOVS*. 2020;61:ARVO Abstract 2199; Petoe MA. *IOVS*. 2019;60:ARVO Abstract 4993), the PRIMA subretinal implant (Pixium Vision),[4] the Orion cortical implant (Second Sight),[5,6] and the suprachoroidal-transretinal stimulation retinal implant (Nidek, Tokyo, Japan).[7] Present-day visual prostheses can produce localizable and spatially distinct phosphenes that can be used to convey useful visual information to the subject,[8] but the visual experience delivered is very crude; fewer than 50% of Argus II and Alpha IMS users tested had a measurable visual acuity in a grating acuity task.[9,10]

Large electrodes (necessitated by safe charge density limits), current spread, and the incidental stimulation of axonal pathways lead to large and irregularly shaped phosphenes and limited spatial discriminability.[11–13] Additionally, non-selective stimulation that activates both "on" and "off" pathways indiscriminantly is likely to have unusual perceptual effects that are not well understood.[14] Novel electrode designs and advances in targeted stimulation strategies offer some promise for future visual prostheses.[15–18] Despite current technical limitations, users of present-day retinal implants have demonstrated improved performance in activities of daily living and in tasks involving navigation, obstacle avoidance, and light localisation (Kolic M. *IOVS*. 2020;61:ARVO Abstract 2199; Petoe MA. *IOVS*. 2019;60:ARVO Abstract 4993).[9,13,19,20]

In addition to spatial and form vision, visual prostheses should also ideally enable the perception of motion. Discrimination of direction of motion has previously been demonstrated in patients implanted with a 24-channel suprachoroidal retinal implant,[13] a subretinal implant,[9,20] and an epiretinal implant.[21] The subjective characteristics of the percepts experienced by participants during these tasks, as well as the particular perceptual cues used to identify motion, has received little attention. One study reported diminished performance when the image-to-electrode mapping was scrambled, demonstrating that retinotopic cues were useful for motion discrimination.[21] However, it remains unclear whether the recipients experience a naturalistic perception of motion. Given the low spatial and temporal resolution of present-day visual prostheses, they might instead perceive a series of discrete flashes that must be consciously interpreted as motion.

In natural vision, direction-selective circuits in the retina and visual cortex compute direction of motion from stimuli that move across the retina, encoding motion for the image-forming pathway, and also effecting oculomotor responses. Direction-selective circuits are important in the generation of smooth pursuit (the regulated eye movements made to maintain fixation on a moving target) and opto-kinetic reflex (a nystagmus that occurs in response to motion across the full visual field, characterised by slow-phase movements in the direction of stimulus motion punctuated by opposing fast-phase movements), both of which act to stabilise moving stimuli on the retina.[22] To our knowledge, the functionality of these circuits under electrical stimulation from a retinal implant has not been investigated.

In the present study we investigated the oculomotor behaviour in response to moving stimuli in recipients of a suprachoroidal retinal implant (Bionic Vision Technologies) with end-stage retinitis pigmentosa. The stimuli were designed to evoke smooth pursuit and optokinetic reflexive eye movements to determine the functionality of retinal and cortical direction-selective circuits under electrical stimulation with the implant. As a corollary, we aimed to reveal the strategies and perceptual cues used by the subjects to determine direction of motion. We categorize the observed eye movements and discuss the implications for prosthetic visual experience.

Methods

Participants

Three subjects (S1, S2, S3) with end-stage retinitis pigmentosa (bare light perception only) participated in the study. These subjects, along with a fourth who did not participate in the present study, were implanted with a 44-channel suprachoroidal retinal implant as part of a two-year longitudinal clinical trial (NCT03406416, February 2018–December 2020). Before implantation none of the participants had measurable visual field remaining (Goldmann kinetic perimetry with target sizes III and V4e). The prosthesis was implanted in the eye with poorer vision at baseline; for S1, this was the left eye, whereas for S2 and S3 this was the right eye. Participant details are summarized in the Table. Device fitting began eight weeks after

Table. Participant Profiles

	S1	S2	S3
Gender	Male	Male	Female
Age at implant (years)	47	63	66
Eye condition	Retinitis pigmentosa (rod cone)	Retinitis pigmentosa (rod cone)	Retinitis pigmentosa (cone rod)
Observed nystagmus	Mild	Intermittent	None
Visual acuity	Light perception OU	Light perception OU	Light perception OU
ffERG stimulus light threshold (cd.s/m^2)	0.1	0.1	0.001
Age when legally blind	20	34	41
Years of useful form vision	34	43	56
Primary mobility aid	Cane	Cane	Guide dog
Implanted eye	Left	Right	Right

ffERG, full-field electroretinography; OU, both eyes.

surgery ("switch-on"), followed by lab-based training and at-home training. The subjects performed a "moving bar" motion discrimination task periodically as part of a suite of outcome assessments, occurring at 17, 20, 32, 44, 56, and 68 weeks after switch-on. Home- and laboratory-based training continued between assessment time points but was not specific to the motion discrimination task. S1 and S2 also performed a "moving grating" motion discrimination task at a single time-point each (S1: 62 weeks after switch-on. S2: 66 weeks after switch-on). The study was approved by the Royal Victorian Eye and Ear Hospital Human Research and Ethics Committee and was carried out in accordance with the tenets of the Declaration of Helsinki with the informed consent of all participants.

Suprachoroidal Retinal Prosthesis

The retinal implant comprised 46 platinum disc electrodes embedded in silicone implanted in the suprachoroidal space, connected via a lead-wire to a pair of subcutaneous stimulators behind the ear. Two larger diameter (2 mm) electrodes were reserved as return electrodes and 44 smaller electrodes (1 mm diameter) were available for stimulation.[23] The infrared ocular images (Spectralis, Heidelberg Engineering Gmbh, Germany) presented in Figure 1 show the placement of the array with respect to the fovea for each subject.

A psychophysical fitting procedure established the optimal stimulation parameters for each individual. This involved selecting the subset of electrodes that produced the optimal experience for the individual. Electrodes were excluded from the configuration if they did not yield a phosphene within safe charge limits (250nC per electrode at a rate of 50 pulses per second, biphasic pulse, 500 μs phase width) (Nayagam DAX. *IOVS*. 2017;58:ARVO Abstract 4204),[24] or if the phosphene was confusing, indistinct, or not easily discriminable from other phosphenes. Any two neighboring electrodes could optionally be operated as a shorted pair to increase the effective surface area and raise the safe charge limit, yielding phosphenes in areas of the retina where single-electrode stimulation did not produce useful phosphenes. The electrodes that were selected for stimulation in each subject are circled in green in Figure 1. The stimulation parameters for each subject were established within the first 10 weeks post switch-on and were then used for all training and at-home use. To maintain consistency and aid in familiarizing the artificial percepts the stimulation parameters for each participant were kept consistent across all tasks and settings for the duration of the clinical trial, except for minor adjustments to charge levels on individual electrodes to account for changes in perceptual thresholds.

Electrode activity was modulated by images captured by a head mounted camera. Camera images were processed using a Lanczos2 antialiasing filter as described in our previous work.[25] A "scrambled" condition was also used in which the same sampling locations were randomly assigned to the electrodes every five seconds to disrupt the spatial structure of the image while maintaining field of view, overall brightness, and number of phosphenes, as described in previous work.[26,27]

Moving Bar Task

Moving stimuli were presented in a four-alternative forced-choice paradigm (4AFC). In each trial a single horizontal or vertical white bar of width 5° swept

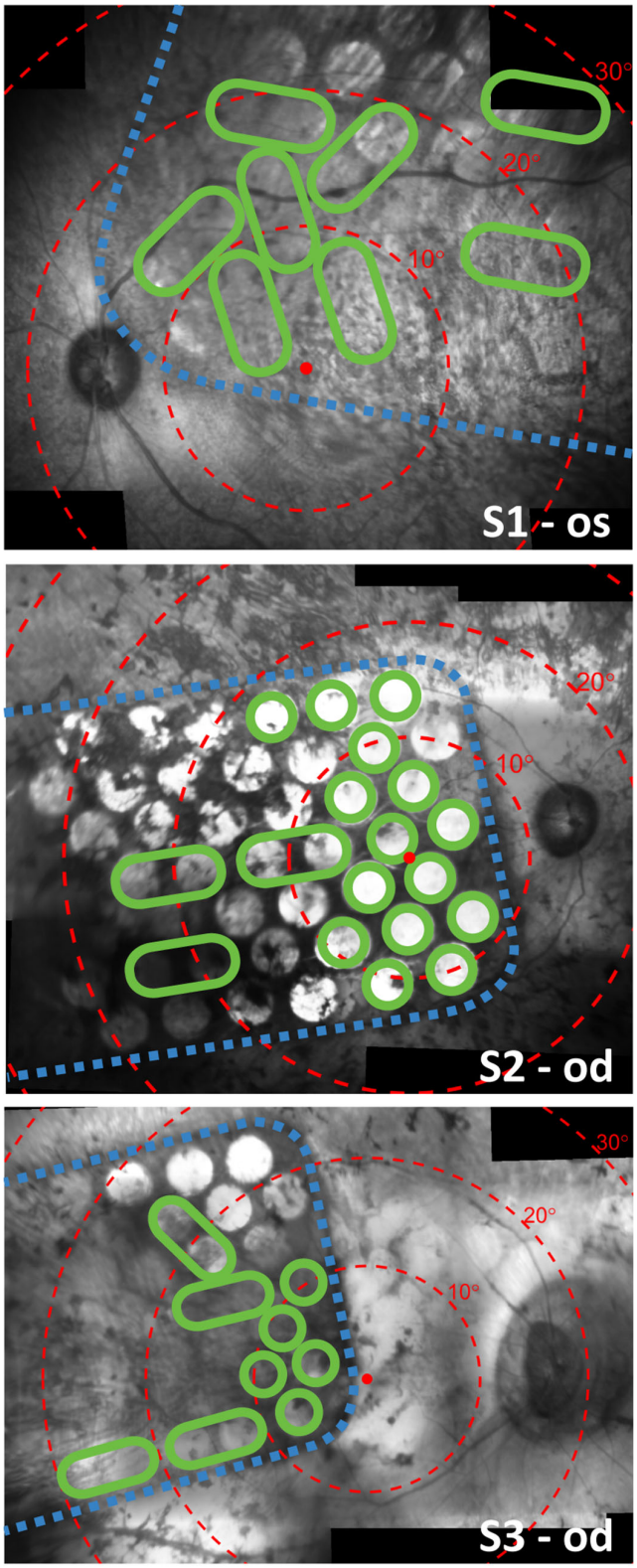

Figure 1. Stitched composite infrared fundus images (Spectralis; Heidelberg Engineering) showing the placement of the array on the retina for S1 (top, 17 weeks after surgery), S2 (middle, eight weeks after surgery), and S3 (bottom, eight weeks after surgery). Electrodes are visible in the images as bright circles. Note that some electrodes are obscured from view due to pigmentation. *Dashed blue lines* trace the edge of the implant. *Red dots* indicate the estimated location of the fovea and concentric *red circles* indicate 10° eccentricities of visual field according to the Drasdo and Fowler schematic eye.[28,29] *Green circles* signify electrodes that were included in the subject's unique stimulus configuration, which was kept constant for all tasks and settings during the clinical trial. Larger *green ovals* indicate that two electrodes were operated as a shorted pair. Electrodes that are not circled in *green* were excluded from the stimulus configuration and were therefore not stimulated during the motion discrimination task. Some optical distortion and stitching artefact is expected.

left, right, up, or down, across a black background on a 42″ monitor viewed at approximately 40 cm distance (approximately 100 × 67° visual arc). The subject's nonimplanted eye was patched. The direction of motion was selected according to a balanced-random schedule. The orientation of the bar was always perpendicular to the direction of motion. The subject's task was to identify the direction of motion and respond by pressing the corresponding key on a keypad. Audio cues signaled the appearance of the bar (trial start) and the acknowledgement of the subject's response. No other feedback was given. Initially the speed of the bar was set to 7°/s and 24 trials per condition were performed with normal vision processing, scrambled vision processing, and with the system off on a balanced-random schedule. Then the speed was increased to 15°/s for an additional 24 trials per condition, and finally to 30°/s for 24 trials per condition. The subjects were not informed of the scrambled condition, anticipating that the device was either turned on or off. The task was repeated at regular intervals during the course of the clinical trial as part of a larger suite of outcome assessments (Kolic M. *IOVS*. 2020;61:ARVO Abstract 2199; Petoe MA. *IOVS*. 2019;60:ARVO Abstract 4993). Subjects could move their head freely, and they were not given any particular instruction regarding eye movement; however, in the course of their training they had been made aware that eye position can affect the locations of phosphenes.

Moving Grating Task

The moving grating task was identical to the moving bar task except the bar stimulus was replaced by a grating stimulus, consisting of regularly spaced parallel white bars. The white bars were 5° in width with a pitch of either 20° or 30° (corresponding to a 15° or 25° gap between neighboring bars). This spacing was selected to be smaller than the device's visual field (Fig. 1) such that at least one bar of the grating was within the sampling region at any given time, while being mindful of the limited visual acuity of the retinal implant. As in the moving bar task, the stimulus moved

in one of the four cardinal directions at random, and the subject was required to determine the direction of motion and respond by pressing a key on a keypad. The stimulus filled the entire monitor and was displayed continuously until a response was logged. Because of time constraints the task was only performed in S1 and S2 in the normal condition.

Eye and Head Tracking

A head-mounted eye tracker (Arrington Research, Scottsdale, AZ, USA) recorded the position of the implanted eye at 60 Hz. Eye position data was processed to remove blink artefact prior to any analysis. Calibration of the system was not possible with nonsighted participants, because the calibration sequence requires the participant to fixate on a number of visual targets. Instead, following the manufacturer guidelines for this scenario, the system was calibrated for a sighted user, and this calibration was then applied during data acquisition in this study. The eye-facing cameras were positioned such that the canthi were aligned with the left and right edges of the image to ensure the size of the eye in the camera image was consistent across all sessions. Small changes in the position of the camera relative to the eye are expected when moving the headset from the sighted user to the nonsighted user, and this can introduce slippage error in the calculated gaze position. However, only relative changes from stimulus onset are analyzed in this study, so small changes in absolute gaze estimates are unlikely to significantly affect the results. Head azimuth and elevation was recorded in degrees at 20 Hz using a magnetic motion tracker (Ascension trakSTAR; Ascension Technology Corporation, Milton, VT, USA). Saccadic eye movements were identified using a velocity threshold of 50°/s. A subset of the data for each subject was visually inspected to verify the robustness of the saccade detection.

The net head movement in each trial of the moving bar and moving grating task was quantified by ΔHead, the aggregate of all head movement made between stimulus onset (first electrode stimulated) and stimulus offset (last electrode activated). Likewise, $\Delta Eye_{saccadic}$ and ΔEye_{drift} respectively quantify the aggregate saccadic and drift (non-saccadic) eye movement between stimulus onset and offset. If an eye movement continued after stimulus offset (eye velocity greater 4°/s) then the sampling time was extended until either the movement ceased (velocity less than 4°/s), the direction of the movement deviated more than 30° from the original movement, or 300 ms after stimulus offset, whichever occurred first. This ensured that any eye movement that began during the period of stimulation was fully captured. The ΔEye and ΔHead vectors were then normalized by subtracting the angle of stimulus motion, such that the normalized ΔEye and ΔHead represented the direction of the eye or head movement relative to the direction of the stimulus.

Statistical Analyses

Mean normalized ΔHead and ΔEye_{drift} were compared against zero to determine whether any significant head movements or drift eye movements congruent to the stimulus direction occurred in the moving bar task (Hotelling's one sample *t*-test with Bonferroni correction for multiple comparisons). Any trial in which the initial eye position was greater than 2 SD from the mean eye position over the entire session was excluded to mitigate any possible effect of an eccentric initial eye position. Nystagmus was identified by comparing the mean $\Delta Eye_{saccadic}$ and ΔEye_{drift} over many trials—whereby drift and saccadic movements with opposing polarities indicated nystagmic eye movement. Behavioral responses from the keypad were compared for significance against chance (25%) using a binomial test with an alpha level of 0.05.

Results

Moving Bar Task Performance

S1 and S2 completed the moving bar task for all three stimulus speeds. S3 attempted the 7°/s stimulus on all assessment dates, the 15°/s stimulus at 20, 30, and 68 weeks post switch-on, and did not attempt the 30°/s stimulus at all because of time constraints. Performance on the task is presented for all subjects in Figure 2. The percentage of correct responses was very consistent between sessions, so data from all sessions was pooled together. For S1 performance in the normal condition was good (61%–67%) and performance in the scrambled condition was worse (47%–23%) but still significantly above chance for 7°/s and 15°/s stimuli ($P < 0.001$). For S2 performance in the normal condition was excellent (83%–87%) but performance in the scrambled condition was not significantly above chance for any stimulus speed. For S3 performance was significantly above chance for in the normal and scrambled conditions for 7°/s stimuli but not for 15°/s stimuli. Performance was not significantly above chance in the system off condition for any participants.

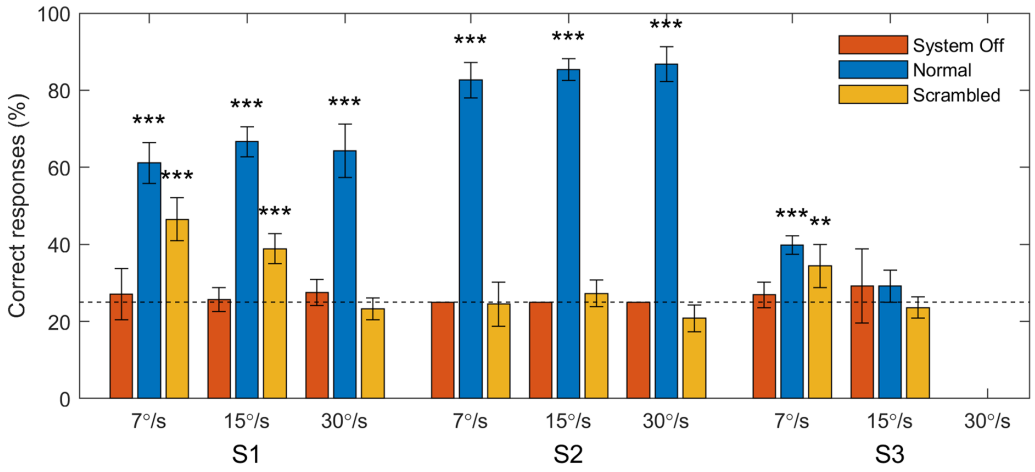

Figure 2. Percent of correct responses for each subject in the moving bar task. Bars represent score pooled across all sessions. *Error bars* represent the standard error of the mean of the score per session. Data are separated by the speed at which the stimulus moved and by the image processing condition (normal, scrambled, system off). The horizontal dotted line specifies the chance rate of 25%. Asterisks denote above-chance performance for data pooled across sessions (binomial test, $^{**}P < 0.01$, $^{***}P < 0.001$).

Stimulus-Related Smooth Pursuit Eye Movements

Stimulus-related drift eye movements were observed for two subjects. Figures 3A and 3B, respectively, show an exemplar eye and head response for a single trial with S1 in which a 30°/s left-moving stimulus was presented. Figures 3C and 3D, respectively, show the mean (±SD) eye and head response for S1 for all trials in which 30°/s left-moving stimuli were presented. Similar data were obtained for S2 and S3 and summarized as vectors of eye and head motion with respect to normalized stimulus direction (Fig. 4).

Figure 4 summarizes the drift eye movements, head motion, and inferred strategy on the task for all participants. Normalized ΔHead and $\Delta\text{Eye}_{\text{drift}}$ vectors and are plotted for each stimulus speed, showing the head movement and drift eye movement relative to the direction of stimulus movement. Vector angles near 0° indicate eye or head movement congruent to the stimulus movement, that is, systematic and repeatable eye and head movements aligned with the stimulus were observed. Circular markers without vector lines denote cases where the mean normalized ΔHead or $\Delta\text{Eye}_{\text{drift}}$ was not significantly different to zero, indicating that either minimal movement occurred or the direction of the movement was not correlated with the direction of stimulus movement. Responses for 15°/s stimuli were not included for S3 because these stimuli were not discriminable by the subject (Fig. 2).

Head movements congruent to the stimulus motion were observed for S1 for 7°/s and 15°/s stimuli, and for S3 for 7°/s stimuli, implying a strategy that used head scanning (Figs. 4G, 4I). No significant head movements were observed for S2 (all stimulus speeds) or S1 for 30°/s stimuli, implying a strategy that used retinotopic information and not head scanning.

S1 and S2 both had significant drift eye movements congruent to the stimulus direction in the Normal condition (Figs. 4A, 4B), but these eye movements did not occur when the retinotopic information was scrambled (Figs. 4D, 4E). These drift eye movements are unlikely to represent the slow phase of nystagmus because of their dependence on the task stimuli. Nor are they likely to represent a vestibulo-ocular reflex, because the head movement was either minimal or was in the same direction as the eye movement. It is therefore probable that these drift eye movements are smooth pursuit. An example of a supposed smooth pursuit waveform (S1, 30°/s left-moving stimulus) is presented in Figure 3A. The eye movement occurring between approximately $t = 0.5$ to 1.5 seconds bears the primary characteristics of a smooth pursuit: a prolonged eye movement at subsaccadic velocities in a direction congruent with a moving stimulus. This response was highly repeatable (average extent of 14.7° ± 5.1°, Fig. 3C).

Characterization of Baseline Acquired Nystagmus

To characterize any baseline acquired nystagmus, $\Delta\text{Eye}_{\text{drift}}$ and $\Delta\text{Eye}_{\text{saccadic}}$ during the system off condition were compared (Fig. 5). Data from all stimulus speeds and directions were pooled under the assumption that the subjects received no visual input during the task (bare-light perception only, no electrical stimu-

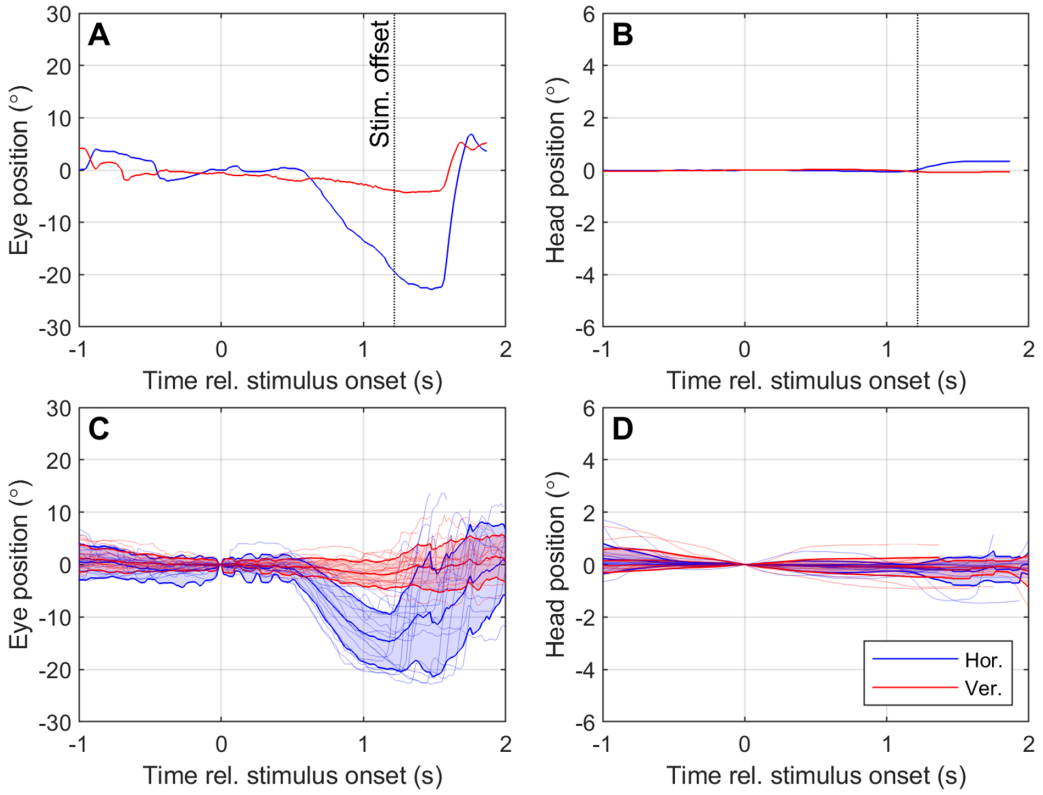

Figure 3. Example of eye and head responses to moving stimuli for participant S1. Panels A and B respectively display the eye and head movement during a single trial in which a 30°/s left-moving stimulus was presented. Panels C and D respectively display the average (± SD) eye and head movement over all trials in which a 30°/s left-moving stimulus was presented and correctly identified. Eye and head position are measured relative to the position at stimulus onset ($t = 0$). Positive values on the y-axis indicate rightwards horizontal movement (*blue lines*) or upward vertical movement (*red lines*). Note that the y-axis scale is different for head movement (B, D) compared to eye movement (A, C) because head movement was minimal.

lation, and resultant performance not significantly greater than chance). No normalization for stimulus direction was performed. Nystagmus is characterized by slow-phase (drift) eye movements punctuated by "beating" fast-phase (saccadic) eye movements in the opposite direction[22], so ΔEye_{drift} and $\Delta Eye_{saccadic}$ movements with opposite polarity would indicate a nystagmus. Figure 5 shows no notable nystagmus for S1, a left-beating nystagmus for S2, and a down-beating nystagmus for S3.

Optokinetic Reflex

Performance using the keypad for the moving grating task for S1 was 50% (30°/s, 20° pitch) and for S2 was 63% (15°/s, 20° pitch), 83% (30°/s, 20° pitch) and 92% (30°/s, 30° pitch). Sawtooth-like waveforms that resembled optokinetic reflex appeared intermittently in the recorded eye position signal during the moving grating task. An example of one such movement is shown in Figure 6A, whereas the mean ΔEye_{drift} and $\Delta Eye_{saccadic}$ are normalized against trial duration and plotted for each subject in Figures 6B and 6C. In healthy vision, the beat (saccadic component) of optokinetic reflex is expected to oppose the direction of stimulus movement.[22] Nystagmic eye movements were identified, but for both subjects the beat was always upward regardless of stimulus direction (Fig. 6). For S2 the severity of nystagmus varied with stimulus direction, but up-beat nystagmus was observed for all moving grating stimuli tested (Fig. 6, only data for 30°/s, 20° pitch are shown). Up-beat nystagmus is inconsistent with either subject's baseline nystagmus (Fig. 5): S1 exhibited no notable nystagmus with system off, and S2 exhibited a left-beating nystagmus.

Discussion

Smooth Pursuit and Nystagmus

In this study we examined the contributions of fast (saccadic) and slow (drift/pursuit) eye movements to overall eye movement in a motion discrimination

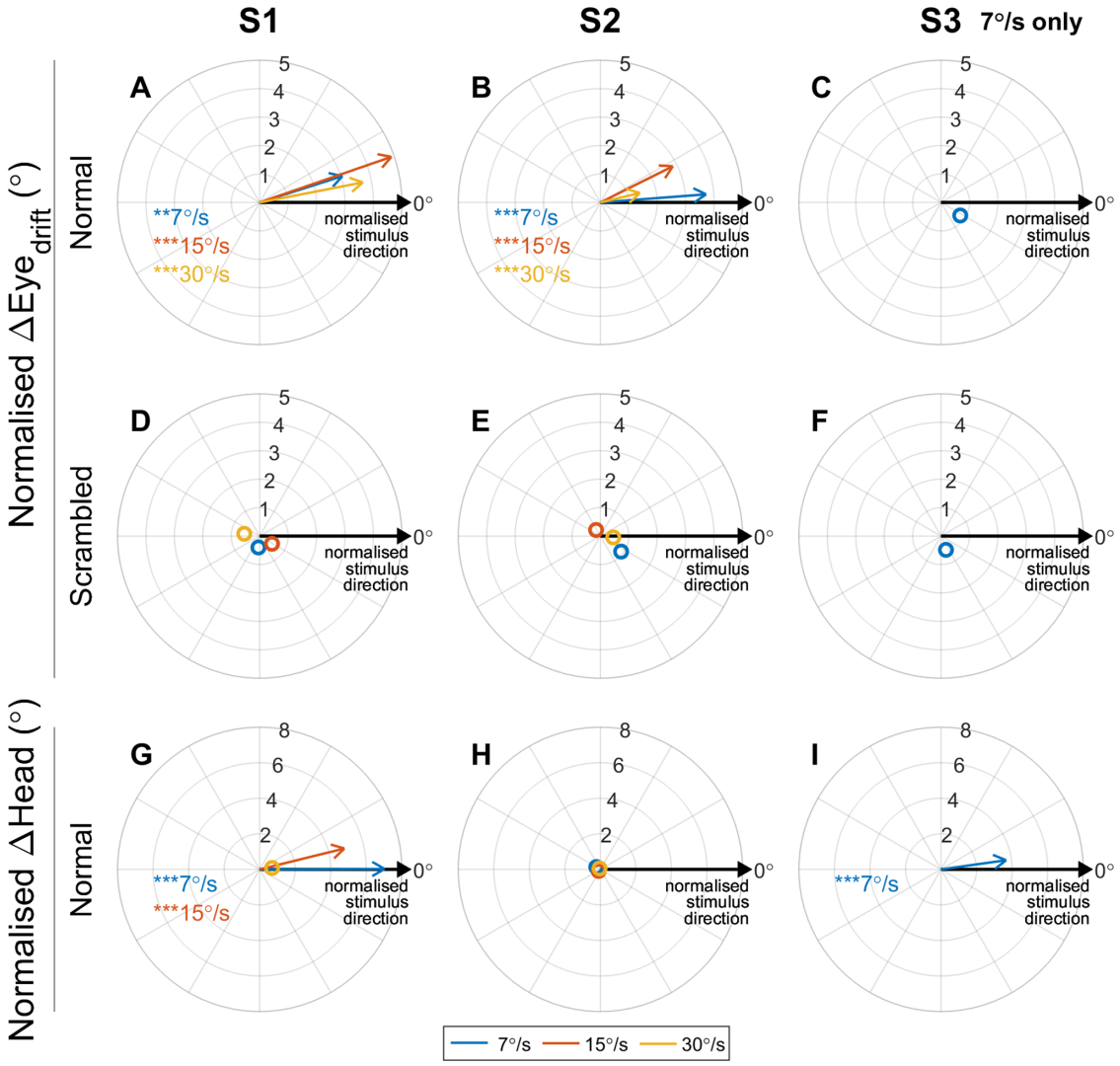

Figure 4. Polar plots displaying the angular error between the direction of motion of the stimulus and the average ΔEye_{drift} and $\Delta Head$ for all subjects in the Normal and Scrambled conditions for 7°/s (*blue*), 15°/s (*red*), and 30°/s (*yellow*) stimuli. Each vector represents the mean direction and magnitude of the eye or head movement relative to the direction of motion of the stimulus. Vectors pointing approximately rightward (0°) indicate that on average the eye or head movement was in the same direction as the stimulus (for all stimulus directions). Asterisks indicate mean eye or head movement was significantly different to zero (Hotelling's one sample *t*-test with Bonferroni correction for multiple comparisons; $*P < 0.05$, $**P < 0.01$, $***P < 0.001$). Hollow markers denote mean eye/head movements that were not significantly different to zero, indicating little movement or nonsystematic movement.

task using prosthetic vision. Our observation that two subjects made smooth pursuit eye movements in the direction of stimulus motion is particularly significant because smooth pursuit generally only occurs in response to a moving visual target. Direction- and orientation-selective circuits in V1, which integrate spatiotemporal patterns of excitation within their receptive fields to encode motion, are necessary for the generation of smooth pursuit in primates and also provide a direction selective input to the image forming pathway.[22,30] A series of discrete flashes could be interpreted as motion in the context of the task, but this would not be expected to elicit a smooth pursuit. Therefore the observation of smooth pursuit in two subjects might suggest the experience of motion was more naturalistic than expected. Both of these two subjects described their experience of motion during the task as "normal."

In the moving grating task two subjects made eye movements that resembled an optokinetic reflex; however, the movement was always up-beat regardless of the direction of stimulus motion. The observed movements are likely to be stimulus-related, rather than acquired nystagmus, because they did not match

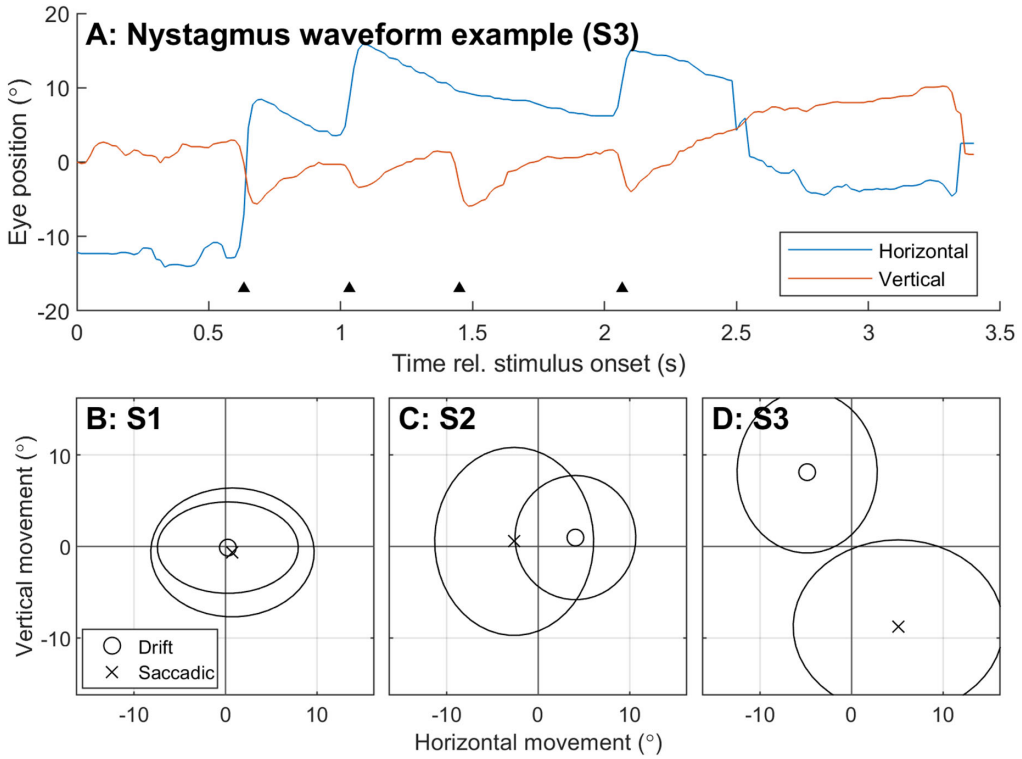

Figure 5. Characterization of baseline acquired nystagmus for each subject using eye movement during the moving bar task in the system off condition. Data was pooled across all stimulus speeds. (A) Example of a nystagmic waveform in S3. *Black triangles* indicate the beat (saccadic component) of the nystagmus. (B–D) Mean ΔEye_{drift} (*circle markers*) is compared to mean $\Delta Eye_{saccadic}$ (*crosses*) for each participant. *Ellipses* indicate standard deviation. Slow and fast phase movements with opposing polarity indicate a beating nystagmus. S1 had no notable nystagmus, S2 exhibited a left-beat nystagmus, and S3 exhibited a down-beat nystagmus.

the earlier characterization of each subject's baseline acquired nystagmus, the degree of nystagmus varied with stimulus direction in one subject, and the subjects were screened before enrollment for neurologic conditions known to cause up-beat nystagmus.

In mammals the optokinetic reflex is modulated by direction-selective retinal ganglion cells that project to the accessory optic system, although the actual direction-selective computation is performed by starburst amacrine cells in the inner retina.[31,32] Given the limited spatial resolution of electrical stimulation with the suprachoroidal retinal implant (1.5 mm electrode pitch), and the fact that suprachoroidal stimulation activates neurons in all retinal layers (likely activating direction-selective retinal ganglion cells directly, regardless of any activation and subsequent computation occurring in the inner retina),[33,34] it is unsurprising that a normal optokinetic reflex was not observed. It is possible that the video processing and electrode sequencing algorithms, which are constrained by the video processing rate (12.5 Hz) and safe stimulation protocols, produced artefact that led to up-beat nystagmus. Alternatively, the significant neural remodeling that occurs in retinal degeneration may have affected the function of the retinal direction-selective circuits and interfered with the generation of the optokinetic reflex.[35] It is unclear what the perceptual effects of such remodeling might be; direction selective retinal ganglion cells are most strongly implicated in optokinetic control and their role in image-forming remains under debate.[36] Further understanding of retinal remodeling and its perceptual and oculomotor effects will be important in establishing a naturalistic integration of retinal implants in late-stage retinal degeneration.

It should also be noted that foveation and image stabilization, the primary purpose of smooth pursuit and optokinetic reflex, is not possible with the present 44-channel suprachoroidal retinal implant. This is due to the decoupling of eye position and camera orientation. The observed smooth pursuit eye movements would not have had the effect of stabilizing the percept, and would in fact have caused further movement of the percept, because eye movements cause movement of phosphenes within the visual field.[37–40] This is also likely to have interfered with the generation of an

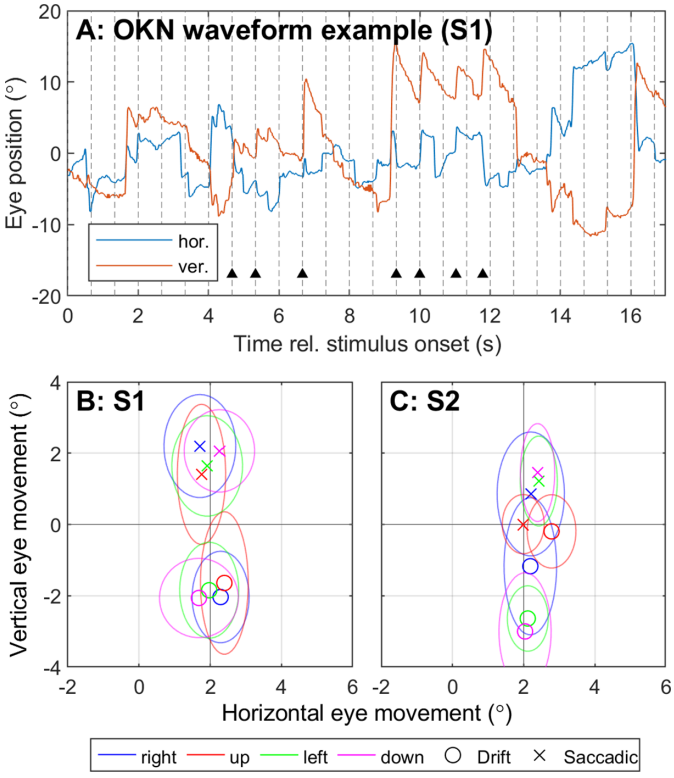

Figure 6. Characterization of nystagmus for S1 and S2 in the moving grating task. (A) Example of a nystagmic waveform observed in S1 during the moving grating task. (B, C) Mean ΔEye_{drift} (*circle markers*) is compared to mean $\Delta Eye_{saccadic}$ (*crosses*) for each stimulus direction for each participant. Color represents the direction of motion of the stimulus. *Ellipses* indicate standard deviation. Slow and fast phase movements with opposing polarity indicate a beating nystagmus. Both participants exhibited up-beat nystagmus in response to the moving grating stimuli, regardless of stimulus direction. Only data for 30°/s, 20° pitch are shown.

optokinetic reflex. Nevertheless, the observation of smooth pursuit movements is an encouraging result for photovoltaic retinal implants or future visual prostheses that incorporate eye position feedback.

The Contribution of Retinotopic Information

Analyses of eye and head movement revealed a range of strategies used in the task. S3 appeared to be the most dependent on head scanning, exhibiting head movements congruent to the stimulus direction and a relatively small decrease in performance when the retinotopic information was scrambled. In contrast, S2 was highly proficient at retinotopic discrimination and made almost no head movement, resulting in excellent performance in the normal condition and chance performance in the scrambled condition. S1 used a mixture of head scanning and retinotopic discrimination—scrambling the retinotopic information diminished performance, but performance remained above chance in cases where head movements were observed (7°/s and 15°/s stimuli). Taken together, these results suggest head position cues were useful when available but that the task was also possible using retinotopic cues only. These results are consistent with published results showing decreased performance in scrambled versus normal for subjects implanted with the Argus II epiretinal implant performing a moving bar task,[21] and for subjects implanted with a 24-channel suprachoroidal retinal implant performing acuity and localization tasks.[13,26]

Array Placement and Stimulation Parameters

Some aspects of the oculomotor response may be explained by the placement of the array on the retina (Fig. 1). In S3, the electrodes that were selected for stimulation span a relatively smaller area of the retina, especially horizontally, which could be impractical for motion detection. This may explain S3's relatively poor performance on the task and apparent reliance on head movement cues. In contrast, S1 had a similar number of active electrodes compared with S3 but performed better in the task, possibly because the active electrodes were more dispersed horizontally. Also in S1, the stimulating electrodes lie superior to the fovea such that phosphenes are expected to appear in the lower hemisphere of the visual field on both the left and right sides. S1 consistently performed worse for up-moving stimuli than any other direction (see response matrix in Supplementary Figure S1), and this was the only stimulus for which smooth eye movements were incongruent with stimulus direction. This may be related to the absence of any electrodes inferior to the fovea and much better coverage of active electrodes horizontally than vertically. In S2, with a sparse electrode mapping in the temporal superior region (Fig. 1), left-moving and down-moving stimuli were the most commonly confused stimuli (Supplementary Figure S1), and the direction of smooth eye movements for those stimuli appeared mostly downward. This was corroborated by the subject, saying the two directions were difficult to distinguish because the lower left of his visual field was unclear.

The results suggest that placing the array squarely over the fovea is optimal, because it provides phosphenes in all quadrants of the visual field. Overall performance in the task also appears to be correlated to the number of active electrodes included in the subject's individual stimulation configuration, which depends on the response of the neurons surrounding each electrode to electrical stimulation within safe limits. Presumably one of the key predictors of performance on the task would therefore be the

integrity of the degenerate retina. The finding that all subjects made significant eye movements, despite understanding that eye movement could be detrimental to their performance, further underscores the need for eye position feedback and image stabilization in camera-based visual prostheses.

Conclusion

Subjects implanted with a 44-channel suprachoroidal retinal implant use a variety of strategies to discriminate direction of motion, with some subjects making use of head position cues and others relying entirely on retinotopic cues. The observation of smooth pursuit eye movements in two subjects indicates some influence of cortical direction-selective circuits under stimulation from the implant, and implies a more naturalistic experience of motion than previously expected. The finding that naturalistic oculomotor responses to moving stimuli can occur even in low-resolution prosthetic vision highlights the potential for eye tracker feedback to improve perceptual localization and image stabilization in camera-based visual prostheses.

Acknowledgments

Supported by the Clive and Vera Ramaciotti Foundation (MAP; Health Investment Grant), the Bertalli Family Foundation to the Bionics Institute, the National Health and Medical Research Council (grant 1082358 to CIA A/Prof Allen), and by the Melbourne Neuroscience Institute Australian Government Research Training Program (SAT). The Bionics Institute and the Centre for Eye Research Australia receive support from the Victorian Government through its Operational Infrastructure Program. DN, MP, ST, KY MK, EB, CA, CL, JK, WK, CW, NB, PA receive(d) funding support from Bionic Vision Technologies.

Disclosure: **S.A. Titchener,** Bionic Vision Technologies Pty Ltd (F); **J. Kvansakul,** Bionic Vision Technologies Pty Ltd (F); **M.N. Shivdasani** (P); **J.B. Fallon,** None; **D.A.X. Nayagam,** Bionic Vision Technologies Pty Ltd (F, P); **S.B. Epp,** Bionic Vision Technologies Pty Ltd (F); **C.E. Williams,** Bionic Vision Technologies Pty Ltd (F, P); **N. Barnes,** Bionic Vision Technologies Pty Ltd (F); **W.G. Kentler,** None; **M. Kolic,** Bionic Vision Technologies Pty Ltd (F); **E.K. Baglin,** Bionic Vision Technologies Pty Ltd (F); **L.N. Ayton,** None; **C.J. Abbott,** Bionic Vision Technologies Pty Ltd (F); **C.D. Luu,** Bionic Vision Technologies Pty Ltd (F, P); **P.J. Allen,** Bionic Vision Technologies Pty Ltd (F, P); **M.A. Petoe,** Bionic Vision Technologies Pty Ltd (F, P)

References

1. Luo YH-L, da Cruz L. The Argus II Retinal Prosthesis System. *Prog Retin Eye Res*. 2016;50:89–107.
2. Edwards TL, Cottriall CL, Xue K, et al. Assessment of the electronic retinal implant alpha AMS in restoring vision to blind patients with end-stage retinitis pigmentosa. *Ophthalmology*. 2018;125(3):432–443.
3. Muqit MMK, Velikay-Parel M, Weber M, et al. Six-month safety and efficacy of the Intelligent Retinal Implant System II device in retinitis pigmentosa. *Ophthalmology*. 2019;126(4):637–639.
4. Palanker D, Le Mer Y, Mohand-Said S, Muqit MMK, Sahel JA. Photovoltaic restoration of central vision in atrophic age-related macular degeneration. *Ophthalmology*. 2020;127(8):1097–1104.
5. Beauchamp MS, Oswalt D, Sun P, et al. Dynamic stimulation of visual cortex produces form vision in sighted and blind humans. *Cell*. 2020;181(4):774–783.e5.
6. Mirochnik RM, Pezaris JS. Contemporary approaches to visual prostheses. *Mil Med Res*. 2019;6(1):1.
7. Fujikado T, Kamei M, Sakaguchi H, et al. One-year outcome of 49-channel suprachoroidal–transretinal stimulation prosthesis in patients with advanced retinitis pigmentosa. *Invest Ophthalmol Vis Sci*. 2016;57(14):6147–6157.
8. Bloch E, Luo Y, da Cruz L. Advances in retinal prosthesis systems. *Ther Adv Ophthalmol*. 2019;11:2515841418817501.
9. Stingl K, Bartz-Schmidt KU, Besch D, et al. Subretinal visual implant alpha IMS–clinical trial interim report. *Vision Res*. 2015;111:149–160.
10. Ho AC, Humayun MS, Dorn JD, et al. Long-term results from an epiretinal prosthesis to restore sight to the blind. *Ophthalmology*. 2015;122(8):1547–1554.
11. Sinclair NC, Shivdasani MN, Perera T, et al. The appearance of phosphenes elicited using a suprachoroidal retinal prosthesis. *Investig Ophthalmol Vis Sci*. 2016;57(11):4948–4961.
12. Beyeler M, Nanduri D, Weiland JD, Rokem A, Boynton GM, Fine I. A model of ganglion axon pathways accounts for percepts elicited by retinal implants. *Sci Rep*. 2019;9(1):9199.

13. Shivdasani MN, Sinclair NC, Gillespie LN, et al. Identification of characters and localization of images using direct multiple-electrode stimulation with a suprachoroidal retinal prosthesis. *Investig Ophthalmol Vis Sci*. 2017;58(10):3962–3974.
14. Fine I, Boynton GM. Pulse trains to percepts: the challenge of creating a perceptually intelligible world with sight recovery technologies. *Philos Trans R Soc B Biol Sci*. 2015;370(1677): 20140208.
15. Sikder MKU, Shivdasani MN, Fallon JB, et al. Electrically conducting diamond films grown on platinum foil for neural stimulation. *J Neural Eng*. 2019;16(6):066002.
16. Zeng Q, Zhao S, Yang H, Zhang Y, Wu T. Micro/nano technologies for high-density retinal implant. *Micromachines*. 2019;10(6):419.
17. Flores T, Huang T, Bhuckory M, et al. Honeycomb-shaped electro-neural interface enables cellular-scale pixels in subretinal prosthesis. *Sci Rep*. 2019;9(1):10657.
18. Chenais NAL, Leccardi MJIA, Ghezzi D. Capacitive-like photovoltaic epiretinal stimulation enhances and narrows the network-mediated activity of retinal ganglion cells by recruiting the lateral inhibitory network. *J Neural Eng*. 2019;16(6):066009.
19. Bloch E, da Cruz L. The Argus II Retinal Prosthesis System. In: *Prosthesis*. London: IntechOpen; 2019.
20. Stingl K, Schippert R, Bartz-Schmidt KU, et al. Interim results of a multicenter trial with the new electronic subretinal implant Alpha AMS in 15 patients blind from inherited retinal degenerations. *Front Neurosci*. 2017;11:445.
21. Dorn JD, Ahuja AK, Caspi A, et al. The detection of motion by blind subjects with the epiretinal 60-electrode (Argus II) retinal prosthesis. *JAMA Ophthalmol*. 2013;131(2):183–189.
22. Purves D, Augustine G, Fitzpatrick D, Hall WC, Lamantia AS, Mcnamara JO. Eye Movements and Sensory Motor Integration. In: *Neuroscience*. Sunderland, MA: Sinauer Associates; 2001:453–468.
23. Ayton LN, Barnes N, Dagnelie G, et al. An update on retinal prostheses. *Clin Neurophysiol*. 2020;131(6):1383–1398.
24. Nayagam DAX, Williams RA, Allen PJ, et al. Chronic electrical stimulation with a suprachoroidal retinal prosthesis: a preclinical safety and efficacy study. *PLoS One*. 2014;9(5):e97182.
25. Barnes N, Scott AF, Lieby P, et al. Vision function testing for a suprachoroidal retinal prosthesis: effects of image filtering. *J Neural Eng*. 2016;13(3):36013.
26. Petoe MA, McCarthy CD, Shivdasani MN, et al. Determining the Contribution of Retinotopic Discrimination to Localization Performance With a Suprachoroidal Retinal Prosthesis. *Investig Ophthalmol Vis Sci*. 2017;58(7):3231–3239.
27. Caspi A, Dorn JD, McClure KH, Humayun MS, Greenberg RJ, McMahon MJ. Feasibility study of a retinal prosthesis: spatial vision with a 16-electrode implant. *Arch Ophthalmol*. 2009;127(4):398–401.
28. Drasdo N, Fowler CW. Non-linear projection of the retinal image in a wide-angle schematic eye. *Br J Ophthalmol*. 1974;58(8):709.
29. Dacey DM, Petersen MR. Dendritic field size and morphology of midget and parasol ganglion cells of the human retina. *Proc Natl Acad Sci*. 1992;89(20):9666–9670.
30. Manning TS, Britten KH. Motion Processing in Primates. In: *Oxford Research Encyclopedia of Neuroscience*. Oxford, UK: Oxford University Press; 2017:1–29.
31. Wei W. Neural mechanisms of motion processing in the mammalian retina. *Annu Rev Vis Sci*. 2018;4:165–192.
32. Taylor WR, Smith RG. The role of starburst amacrine cells in visual signal processing. *Vis Neurosci*. 2012;29(1):73–81.
33. Abramian M, Lovell NH, Morley JW, Suaning GJ, Dokos S. Activation of retinal ganglion cells following epiretinal electrical stimulation with hexagonally arranged bipolar electrodes. *J Neural Eng*. 2011;8(3):35004.
34. Ayton LN, Blamey PJ, Guymer RH, et al. First-in-human trial of a novel suprachoroidal retinal prosthesis. *PLoS One*. 2014;9(12):e115239.
35. Marc RE, Jones BW, Watt CB, Strettoi E. Neural remodeling in retinal degeneration. *Prog Retin Eye Res*. 2003;22(5):607–655.
36. Cruz-Martín A, El-Danaf RN, Osakada F, et al. A dedicated circuit links direction-selective retinal ganglion cells to the primary visual cortex. *Nature*. 2014;507(7492):358–361.
37. Titchener SA, Shivdasani MN, Fallon JB, Petoe MA. Gaze Compensation as a Technique for Improving Hand–Eye Coordination in Prosthetic Vision. *Transl Vis Sci Technol*. 2018;7(1):2.
38. Caspi A, Roy A, Wuyyuru V, et al. Eye movement control in the Argus II retinal-prosthesis enables reduced head movement and better localization precision. *Invest Ophthalmol Vis Sci*. 2018;59(2):792–802.

39. Caspi A, Roy A, Dorn JD, Greenberg RJ. Retinotopic to Spatiotopic Mapping in Blind Patients Implanted With the Argus II Retinal Prosthesis. *Investig Ophthalmol Vis Sci*. 2017;58(1):119–127.

40. Sabbah N, Authié CN, Sanda N, Mohand-Said S, Sahel J-A, Safran AB. Importance of Eye Position on Spatial Localization in Blind Subjects Wearing an Argus II Retinal Prosthesis. *Investig Ophthalmol Vis Sci*. 2014;55(12):8259–8266.